Breaking diffusion coefficient limitation of Bismuth oxide anodes for aqueous alkaline batteries with ultra-high rate capability

Fengming Zhou[a][§], Xiaodong Wang[a][§], Shiyu Gu[a,b], Mingjie Li[a], Ranqiang Xia[a,c], Xinyu Li[a], Zhenjiang Li[a], Qi Zhang[a], Zhenyu Xiao[a*], Lei Wang[a*]

[a] International Cooperation United Laboratory of Eco-chemical Engineering and Green Manufacturing, College of Chemistry and Molecular Engineering, Qingdao University of Science and Technology, Qingdao 266042, P. R. China.

[b] Technology Innovation Center of Battery Safety and Energy Storage Technology, Qingdao, International Science and Technology Cooperation Base of Qingdao, College of Environment and Safety Engineering, Qingdao University of Science and Technology, Qingdao 266042, P. R. China.

[c] Sunvim Group Co.Ltd, Gaomi 261500, P. R. China.

E-*mail:* inorgxiaozhenyu@163.com (Zhenyu Xiao); inorchemwl@126.com (Wang Lei)

Electrochemical measurement

The positive electrode is prepared by mixing the positive samples (80 wt%), acetylene black (10 wt%) and polytetrafluoroethylene (PTFE) (10 wt%) in a ethanol solvent to form a homogeneous slurry. Then, the suspension is then dried in an oven overnight to obtain a black paste. Weigh the paste 2.5 mg (sample mass 2 mg) between two pieces of 1*2 cm nickel foam and ensure that the black paste covers half of the nickel foam area. Finally, the nickel foam was placed under the manual tablet press and kept for 5 s at a pressure of 10 Mpa.

The energy density is obtained by the total loading mass (3.0 mg; positive electrode: 2.0 mg, negative electrode: 1.0 mg). The related detail is as follows:

Firstly, the posivie and negative electrodes of H-Ni(OH)$_2$//A-Bi$_2$O$_3$ device are matched, according to the charge balance equation:

$$C_+ \Delta m_+ = C_- \Delta m_-$$

where C_+ and C_- (mAh/g) are the specific capacity of positive and negative electrodes at a 1 A g^{-1} current density of three electrodes, respectively; Δm_+ and Δm_- (g) are the mass of positive and negative active material, respectively. The optimum mass ratio of positive and negative is calculated to be 1:2. Then, the H-Ni(OH)$_2$//A-Bi$_2$O$_3$ device with the active masses of the positive and negative electrodes are 2.0 and 1.0 mg are fabricated. So the total active mass of the H-Ni(OH)$_2$//A-Bi$_2$O$_3$ device is 3.0 mg, and the related current density of 1, 2, 4, 6, 8,10 A g^{-1}, are performed at 3, 6, 12, 18, 24 and 30 mA, respectively.

Finally, the energy density of H-Ni(OH)$_2$//A-Bi$_2$O$_3$ device is calculated by the following equations:

$$E = \frac{I}{m} \int_{t2}^{t1} V$$

where V (V), and t_1, t_2 (s) represent voltage window and discharge time, respectively.

Electrochemical properties of the single electrode are investigated using a standard three-electrode system. The A-Bi$_2$O$_3$ and H-Ni(OH)$_2$ are used as the working electrodes, Pt wire is used as the counter electrode, and Hg/HgO is used as thereference electrode. The electrochemical analysis of the H-Ni(OH)$_2$//A-Bi$_2$O$_3$ is conducted using a two-electrode system. Electrochemical measurements, such as cyclic voltammetry (CV), galvanostatic charge–discharge (GCD) as well as electrochemical impedance spectroscopy (EIS), were carried out using an electrochemical workstation (DH 7000,Shanghai Chenhua Instrument Co., Shanghai, China) at roomtemperature with 6 mol KOH as the electrolyte.

All chemicals are analytical grade and were used without any purification. Powder X-ray diffraction patterns of the prepared samples are collected on a Rigaku D-MAX2500/PC advance instrument with Cu-Kα radiation (λ = 1.5418 Å). The XPS spectrum of NFS-3 is measured by Thermo Scientific 250xl. The morphology and structure of the prepared samples are examined by electron microscopy (SEM, Zeiss merlin; TEM, FEI Tecnai G2 F20).

Figure
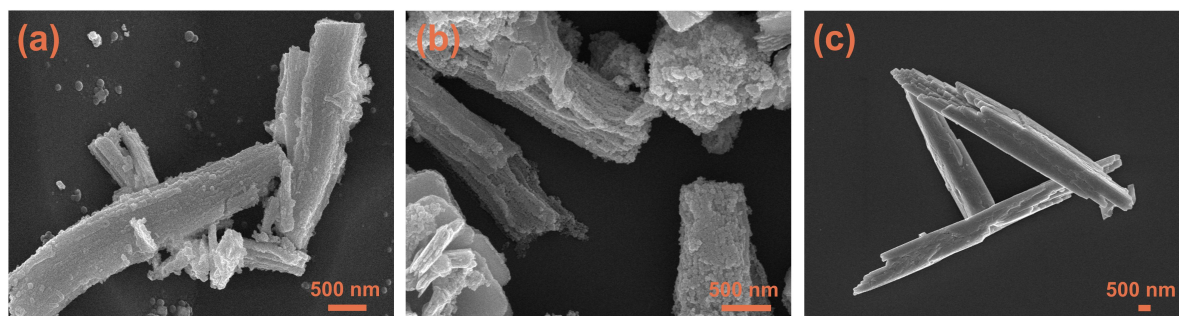
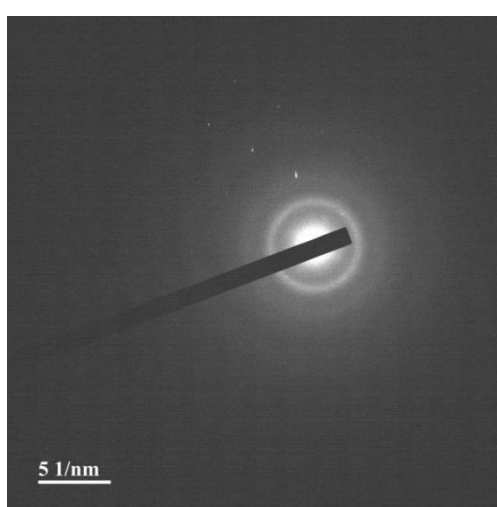Fig. S1 SEM image of Bi_2O_3-0.5M (a); Bi_2O_3-1M (b); Bi_2O_3-6M (c).
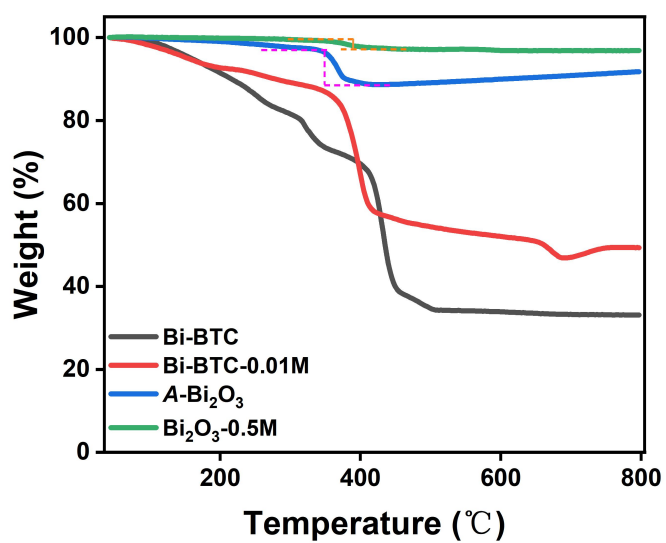

Fig. S2. SEAD image of A-Bi_2O_3.

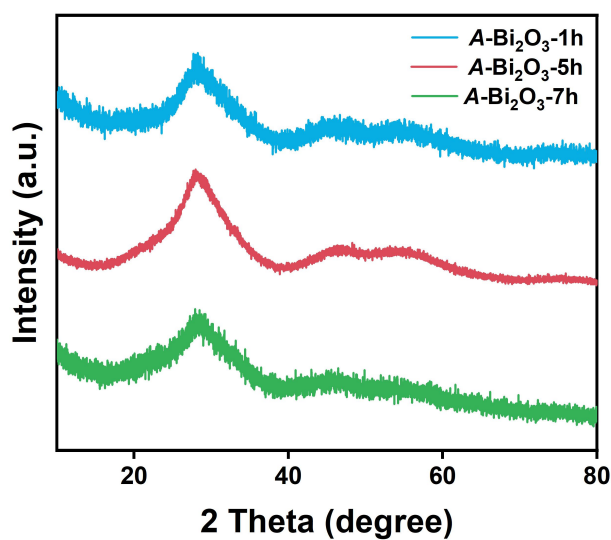Fig. S3. The TGA curves of Bi-BTC, Bi-BTC-0.01M, A-Bi_2O_3 and

Bi$_2$O$_3$-0.5M.

Fig. S4. The XRD curves of *A*-Bi$_2$O$_3$-1h, *A*-Bi$_2$O$_3$-5h and *A*-Bi$_2$O$_3$-7h.
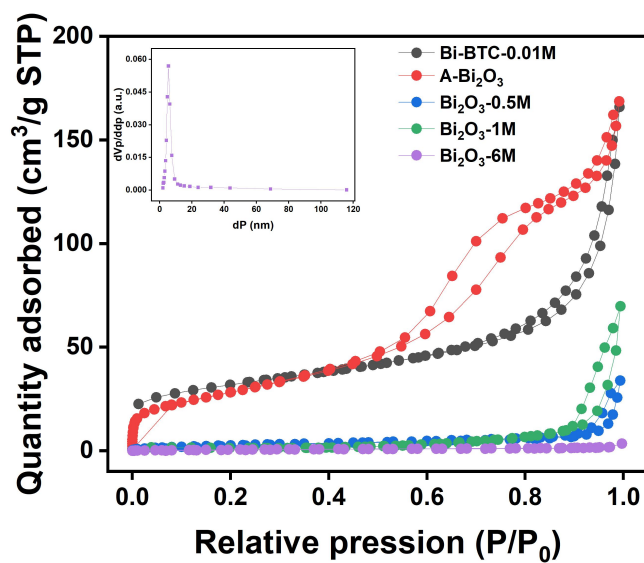
Fig. S5 N$_2$ adsorption-desorption isotherms of Bi-BTC, Bi-BTC-0.01M, *A*-Bi$_2$O$_3$, Bi$_2$O$_3$-0.5M, Bi$_2$O$_3$-1M, and Bi$_2$O$_3$-6M measured at 77K; inset: the corresponding pore size distribution of *A*-Bi$_2$O$_3$.
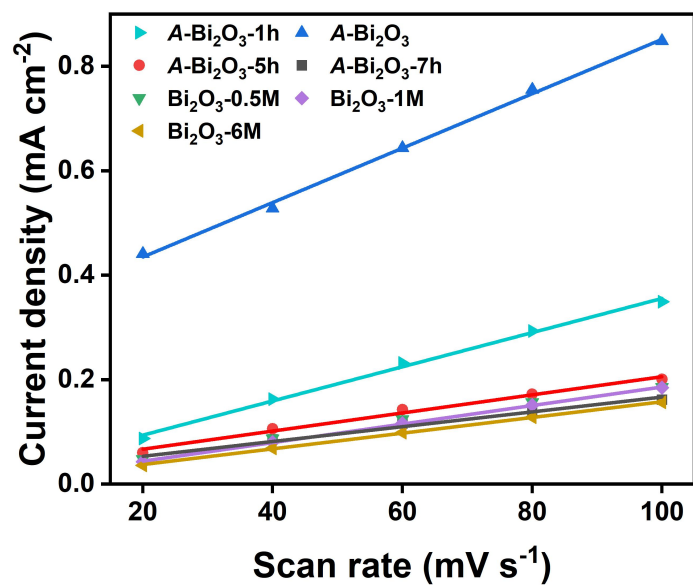
Fig. S6. C_{dl} curves of samples.
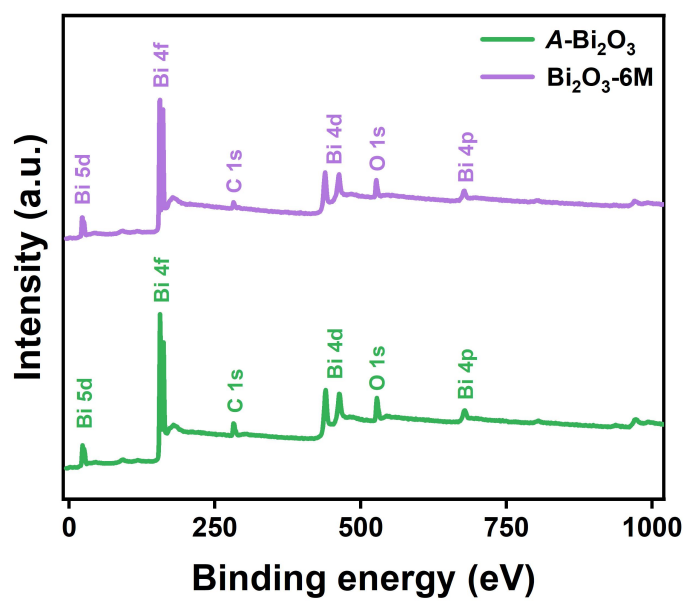
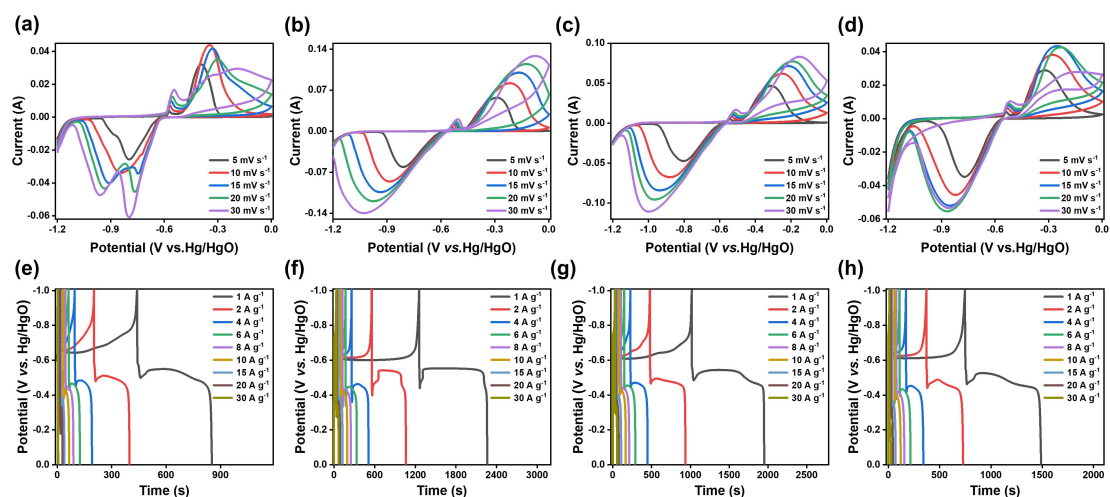Fig. S7 The full spectrum XPS spectra of the A-Bi$_2$O$_3$ and Bi$_2$O$_3$-6M.

Fig. S8 CV curves of (a) Bi-BTC-0.01M; (b) Bi_2O_3-0.5M; (c) Bi_2O_3-1M; (d) Bi_2O_3-6M; GCD curves of (e) Bi-BTC-0.01M; (f) Bi_2O_3-0.5M; (g) Bi_2O_3-1M; (h)Bi_2O_3-6M.
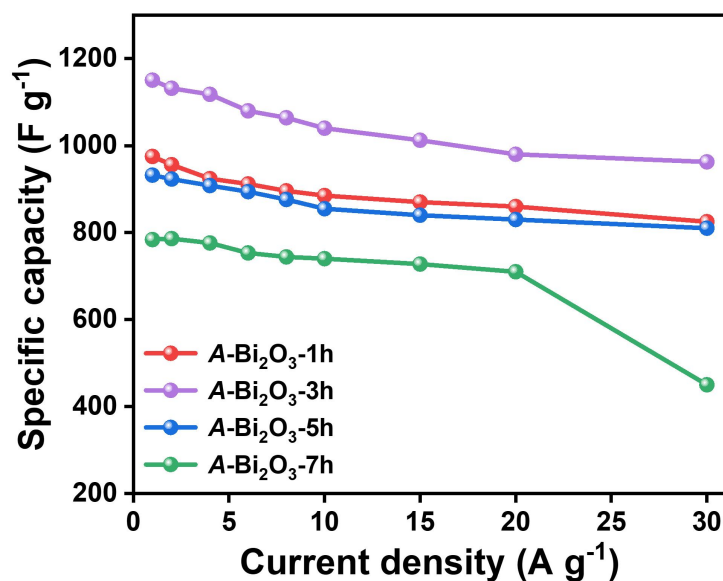
Fig. S9 Specific capacitance of A-Bi_2O_3-1h, A-Bi_2O_3-3h, A-Bi_2O_3-5h, and A-Bi_2O_3-7h at different densities.
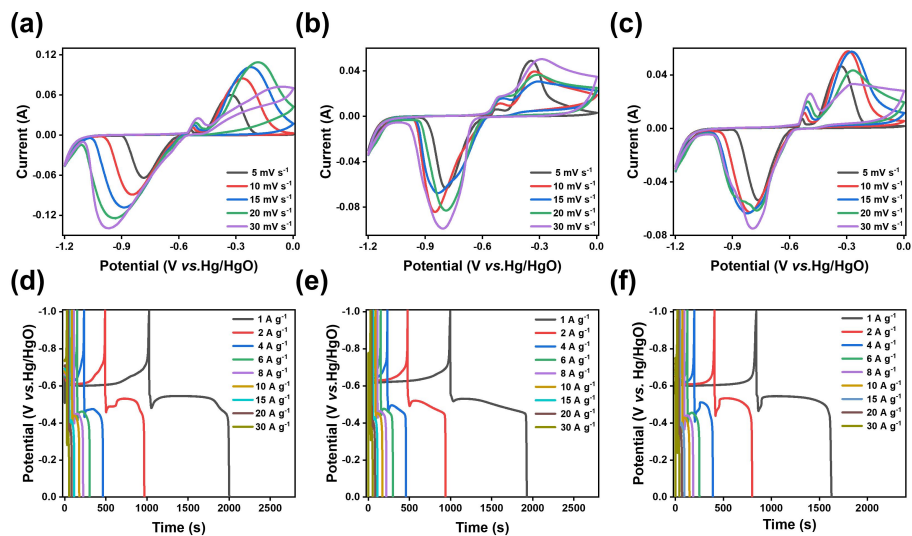
Fig. S10 CV curves of (a) A-Bi_2O_3-1h; (b) A-Bi_2O_3-5h; (c) A-Bi_2O_3-7h; GCD curves of (d) A-Bi_2O_3-1h; (e) A-Bi_2O_3-5h; (f) A-Bi_2O_3-7h.
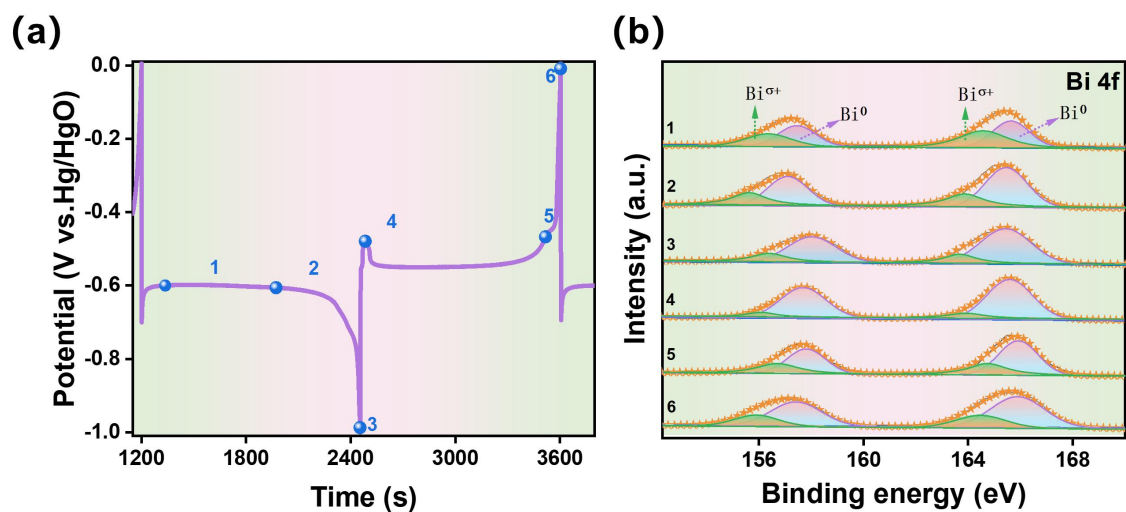

Fig. S11 (a) charge/discharge curve of A-Bi_2O_3 electrode in KOH (6 M) at 1 A g^{-1} ; (b) Ex situ XPS patterns.
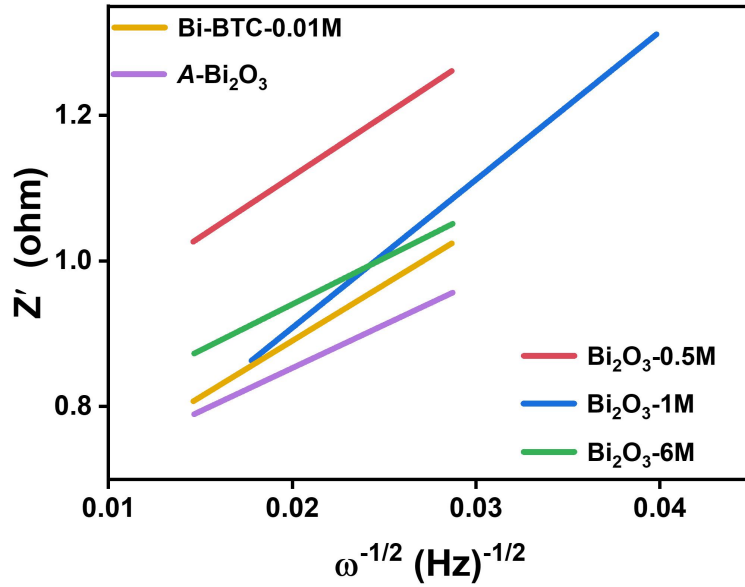
Fig. S12 The Z' of Bi-BTC-0.01M, A-Bi$_2$O$_3$, Bi$_2$O$_3$-0.5M, Bi$_2$O$_3$-1M, and Bi$_2$O$_3$-6M varies with $\omega^{-1/2}$ at low frequency section.
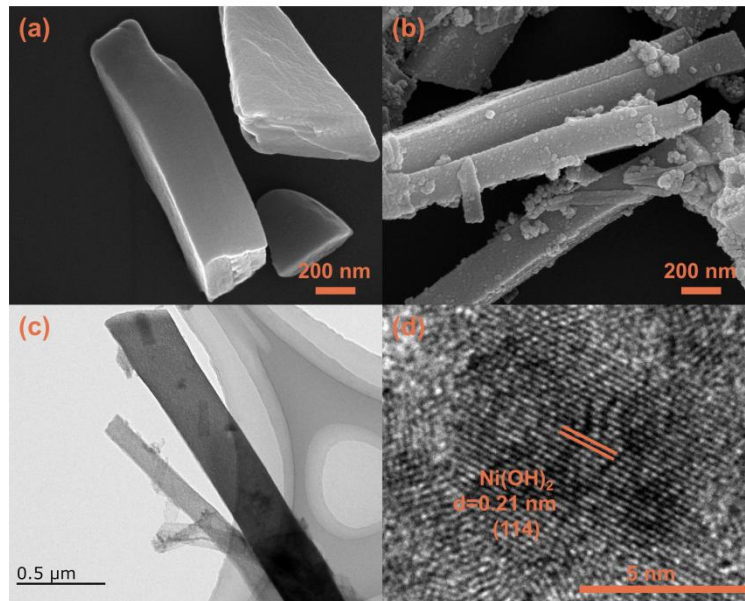

Fig. S13 SEM image of Ni-BTC (a); H-Ni(OH)$_2$ (b); TEM image of H-Ni(OH)$_2$ (c); HRTEM image of H-Ni(OH)$_2$ (d).
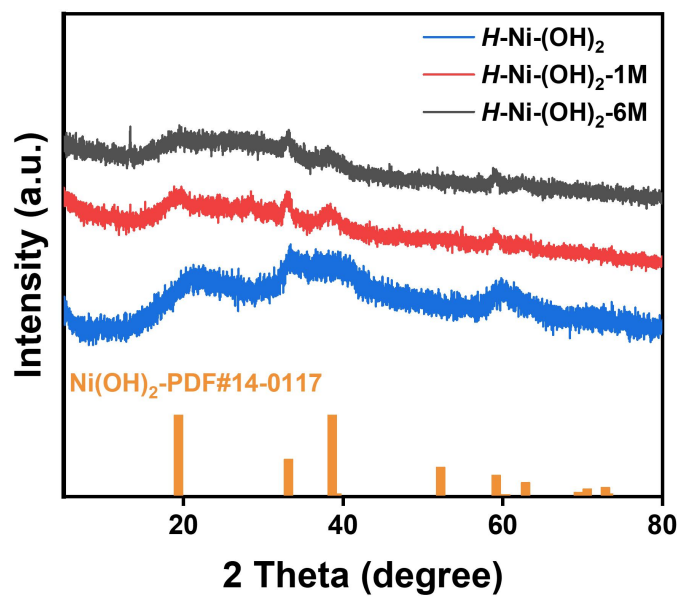
Fig. S14 XRD of *H*-Ni(OH)$_2$, *H*-Ni(OH)$_2$-1M, and *H*-Ni(OH)$_2$-6M.
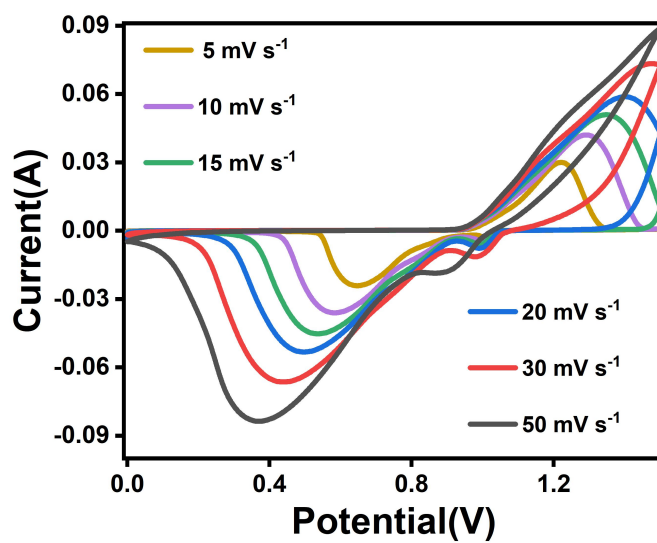
Fig. S15 CV curves of *H*-Ni(OH)$_2$//*A*-Bi$_2$O$_3$ AAB.
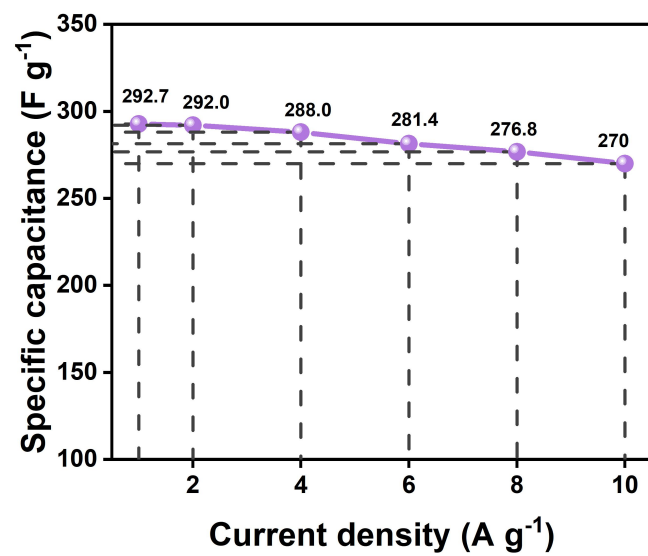
Fig. S16 Specific capacitance of *H*-Ni(OH)$_2$//*A*-Bi$_2$O$_3$ AAB at different densities.

Table

Tab. S1 The BET surface area of different samples.

Sample	BET surface area ($m^2\ g^{-1}$)
Bi-BTC-0.01M	107.5
A-Bi$_2$O$_3$	104.7
Bi$_2$O$_3$-0.5M	10.9
Bi$_2$O$_3$-1M	24.6
Bi$_2$O$_3$-6M	2.6

Tab. S2 The ECSA values of different samples.

Samples	C_{dl}	ECSA (cm^2)
Bi-BTC MOF	1.73	0.035
Bi BTC-0.01M	2.62	0.044
A-Bi$_2$O$_3$	5.21	0.087
Bi$_2$O$_3$-0.5M	3.17	0.053
Bi$_2$O$_3$-1M	1.78	0.030
Bi$_2$O$_3$-6M	1.50	0.025
A-Bi$_2$O$_3$-1h	3.27	0.055
A-Bi$_2$O$_3$-5h	1.74	0.029
A-Bi$_2$O$_3$-7h	1.42	0.024

Tab. S3 The values of σ and D of different samples.

Sample	σ	D (cm^2/s)
Bi-BTC-0.01M	15.43	4.97×10^{-11}
A-Bi$_2$O$_3$	11.87	8.40×10^{-11}
Bi$_2$O$_3$-0.5M	12.67	7.37×10^{-11}
Bi$_2$O$_3$-1M	16.68	4.25×10^{-11}
Bi$_2$O$_3$-6M	20.36	2.85×10^{-11}